

# SENZORI DE GAZ ÎN SISTEMUL BINAR SnO<sub>2</sub> – ZrO<sub>2</sub>

## GAS SENSORS IN SnO<sub>2</sub> – ZrO<sub>2</sub> BINARY SYSTEM

**ȘTEFANIA STOLERIU, ANAMARIA PUIA, SORIN ION JINGA\*, ECATERINA ANDRONESCU**

*Universitatea POLITEHNICA București, Str. G. Polizu nr. 1, 011061, București, România*

*The paper's aim is to present the preparation and characterization of ceramic sensors in SnO<sub>2</sub>-ZrO<sub>2</sub> binary system, using nanopowders obtained through co-precipitation from the corresponding chlorides.*

*All nanopowders were characterized by X-ray diffraction (XRD) and transmission electron microscopy (TEM). The XRD results show specific diffraction lines of tin oxide solid solutions and tetragonal zirconia solid solutions. The TEM examination shows particle size being below 10 nm with tendency of agglomeration in large agglomerates.*

*For ceramic sensors obtaining, the nanopowders were shaped and thermally treated in air for sintering, at temperatures between 900° and 1300°C, for 2 hours.*

*In order to determine the sensitivity of ceramic sensors, the electrical resistance was measured in air, in methane saturated atmosphere and in methanol vapor saturated atmosphere, as well. The obtained sensors are more sensitive to methanol than to methane, the compositions with a higher amount of tin oxide showing higher sensitivity values to both methanol and methane.*

*Scopul lucrării îl reprezintă obținerea și caracterizarea unor senzori ceramici care aparțin sistemului binar SnO<sub>2</sub>-ZrO<sub>2</sub>, folosind nanopulberi obținute prin metoda co-precipitării, din cloruri metalice corespunzătoare.*

*Toate nanopulberile au fost caracterizate prin difracție de raze X și prin microscopie electronică de transmisie. Spectrele de difracție prezintă linii specifice soluțiilor solide de oxid de staniu și, respectiv de oxid de zirconiu. Imaginele TEM pun în evidență particule cu dimensiuni sub 10 nm, cu o tendință de aglomerare în agregate foarte mari.*

*Pentru obținerea senzorilor ceramici, nanopulberile au fost fasonate și sinterizate în aer, la temperaturi cuprinse între 900° și 1300°C, pentru 2 ore.*

*Sensibilitatea senzorilor ceramici a fost determinată prin măsurarea rezistențelor electrice în aer, în atmosferă saturată în metan și în atmosferă saturată de vapori de metanol. Senzorii cercetați au fost mult mai sensibili față de metanol, comparativ cu metanul. Senzorii cu cantitatea cea mai mare de oxid de staniu, prezintă cea mai mare sensibilitate atât față de metanol cât și față de metan.*

**Keywords:** ceramic sensors, tin oxide, sensitivity, nanopowders

### 1. Introduction

Environmental monitoring constitutes one of the major concerns of civil and industrial applications. In the near future, it is predicted the use on a larger scale of sensors, devices made from low-cost materials, stable in time and resistant to environmental factors.

Among all categories of sensors, those which signal assess and monitor the presence of gases are of particular importance. In this context, sensors based on oxide materials occupy a special place, in particular, due to their chemical resistance and the high temperature range in which they can be used.

Oxides are the most often used materials, because of their great mechanical and chemical resistance and especially their refractoriness. The main drawback consists in the difficulty of processing. They have normal densities, linear expansion of  $10^{-6}$  magnitude and thermal conductivity of 0.025 J/cm·K at 200°C [1]. The metal oxides are interesting materials for basic research and technological applications due to their

wide variety of electronic and chemical properties. Among these, is to be found tin dioxide (SnO<sub>2</sub>), which belongs to a class of materials that combine high electrical conductivity with optical transparency, making it suitable for optoelectronic applications [2].

A wide range of oxides presents sensitivity in terms of oxidation or reduction of gases, by varying their electrical properties, but the first oxide considered was SnO<sub>2</sub> and still is the most commonly used for such applications. Evidently, there is a strong relationship between the gas sensitivity of oxides and their surface chemical activity. In most applications, tin dioxide is rarely used in its pure form and usually is being modified through contamination by doping or other additives. Understanding the influence of additives on their properties is very important [3-4].

Tin dioxide is a n-type semiconductor, with a wide band gap of 3.6 eV and it is frequently used due to its stability and its high carrier density and high concentration of intrinsic vacancies and stoichiometry-altering vacancies, correlated with its

\* Autor corespondent/Corresponding author,  
Tel.: +40 21 402 9049, e-mail: [sorinionjinga@yahoo.com](mailto:sorinionjinga@yahoo.com)

electrical conductivity. Tin dioxide shows a big scientific interest due to the wide range of its possible applications [5].

Zhaojia Wang and others [6] observed the effect of doping with zirconium dioxide upon the selectivity of  $\text{SnO}_2$  nano-wires. It was found that the sensor exposed to alcohol shows an enhanced response with zirconia amount increasing, the peak being reached for the 15 mol% sample. Guojia Fang [7] presented that  $\text{ZrO}_2\text{-SnO}_2$  thin films obtained by sol-gel from non-alkoxydes precursors exhibit a good sensitivity, high selectivity and high response time. The susceptibility to gases of  $\text{SnO}_2$  thin films is improved by doping with  $\text{ZrO}_2$ , while the detection temperatures are decreased in the lower temperature range [8].

## 2. Experimental

Present paper is aimed, as main objective, to the obtaining and investigation of the tin oxide - zirconia ceramics sensors with respect to the sensing properties, in a general compositional frame.

As a first step, nanopowders were obtained via co-precipitation, from  $\text{ZrCl}_4$  and  $\text{SnCl}_2\cdot 2\text{H}_2\text{O}$  analytically pure.

Four different oxide composition where synthesized, as shown in Table 1.

Table 1

Oxide composition of the studied samples  
*Compoziția oxidică a probelor studiate*

	Z2S8	Z4S6	Z6S4	Z8S2
$\text{ZrO}_2$ (%)	20	40	60	80
$\text{SnO}_2$ (%)	80	60	40	20

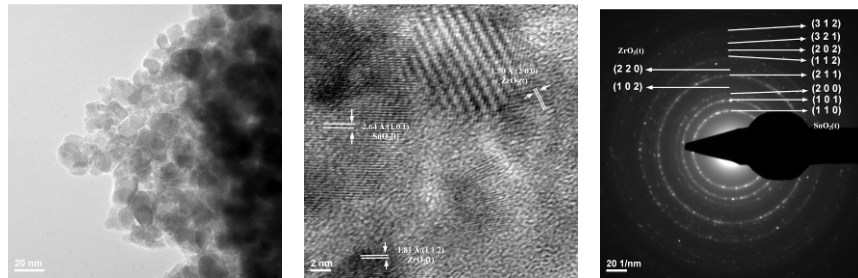


Fig. 1. TEM images of Z2S8 sample //Imagini MET ale probei Z2S8.

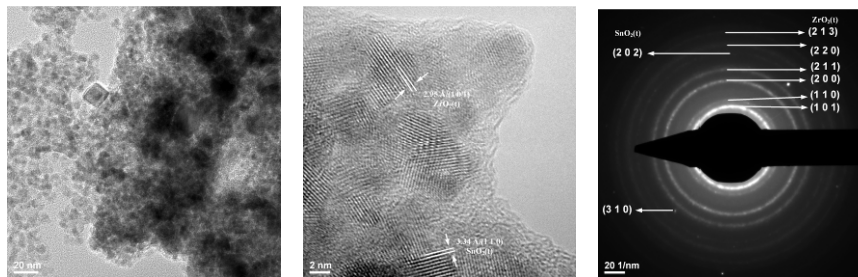


Fig. 2 - TEM images of Z4S6 sample / *Imagini MET ale probei Z4S6*.

The raw materials were dissolved in distilled water and precipitated at  $\text{pH} = 12$  (achieved by adding ammonia solution). The obtained precipitates were filtered and washed until complete removal of chloride ions. The samples were dried for 24 hours at a temperature of  $60^\circ\text{C}$  and then calcined at  $350^\circ\text{C}$ .

After calcination, the powders were characterized and shaped into cylinders (with 8 mm diameter and 4 mm height) by uniaxial pressing. The obtained samples were thermal treated in air, for sintering, at temperatures of  $900^\circ$ ,  $1000^\circ$ ,  $1100^\circ$ ,  $1200^\circ$ , and  $1300^\circ\text{C}$ , for 2 hours.

## 3. Characterization of the obtained nanopowders

All obtained and calcined powders were subject to X-ray diffraction (using Shimadzu XRD 6000 X-ray diffractometer) and high-resolution transmission electron microscopy (HRTEM, using Tecnai G<sup>2</sup> F30 S-TWIN).

### 3.1. Transmission electron microscopy analysis

The samples calcined at the temperature of  $350^\circ\text{C}$  were investigated by transmission electron microscopy (Figure 1- Figure 4). It was concluded that all studied powders are situated within nanoscale range.

The obtained powders can be classified as nanoparticles, the particle size distributions having a characteristic diameter below 10 nm. It can be also noted the nanoparticles tendency of agglomeration in large agglomerates (larger than 30- 40 nm).

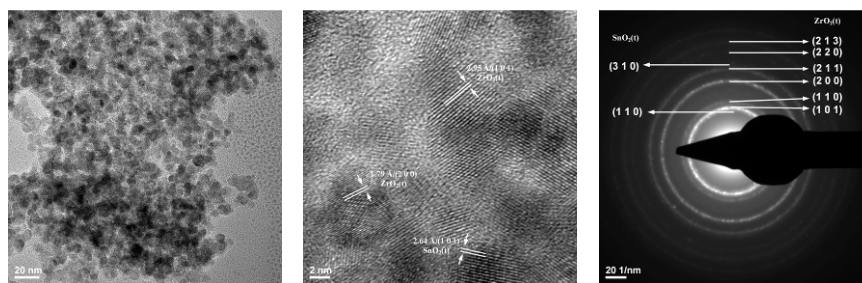


Fig. 3 - TEM images of Z6S4 sample / Imagine MET ale probei Z6S4.

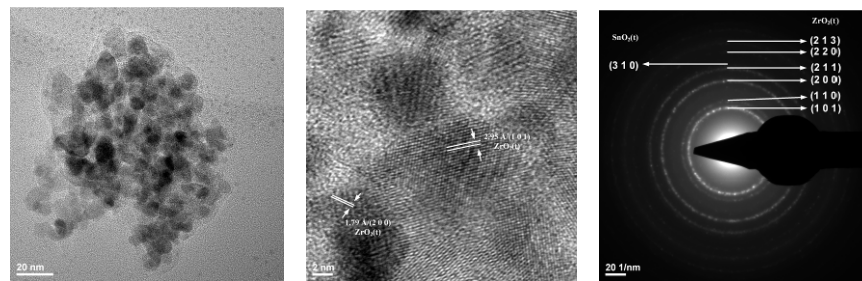


Fig. 4 - TEM images of Z8S2 sample/ Imagine MET ale probei Z8S2.

The crystalline degree seems more pronounced for the sample with 80%  $\text{SnO}_2$ .

The selected-area diffraction pattern for the obtained samples indexes to tin oxide and tetragonal zirconia, in agreement with the X-ray diffraction data (Figure 5).

### 3.2. Diffraction analysis

The samples calcined at 350°C have undergone X-ray diffraction test and the recorded spectra are shown in Figure 5.

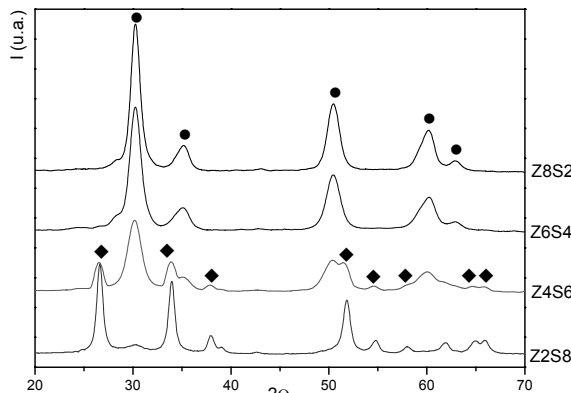


Fig. 5 - X-ray diffraction analysis of the samples calcined at 350°C / Analize de difracție de raze X ale probelor calcinate la 350°C.

(● -  $\text{ZrO}_2$  tetragonal (ASTM 79-1679); ◆ -  $\text{SnO}_2$  (ASTM 01-0657)).

In the X-ray diffraction spectra of corresponding calcined powders, specific peaks of nanopowders can be observed, the specific diffraction lines of tin oxide solid solutions, and tetragonal zirconia solid solutions can be identified respectively. For the end member mixtures there was detected only one type of solid solution, being

obvious the ability of tin oxide to form solid solution with zirconia.

The shape of the peaks also suggests the nanometric particle size of the obtained samples.

## 4. Characterization of ceramic sensors

### 4.1. Diffraction analysis

X-ray diffraction analyses were performed for the sintered samples and the obtained spectra are shown in Figure 6.

The X-ray diffraction spectra of the sintered samples reveal the presence of maximum three phases, depending on composition. For zirconia-rich samples, specific peaks of  $\text{SnO}_2$  solid solutions are not detected, due to a possible complete integration of  $\text{SnO}_2$  in  $\text{ZrO}_2$  lattice, forming tetragonal and cubic zirconia solid solutions.

For  $\text{SnO}_2$ -rich samples, it can be observed the presence of cubic solid solution over a wide temperature range; the increase of the crystalline degree leads to a decrease in the ability of forming cubic solid solutions.

### 4.2. Microscopic analysis

The obtained ceramic materials were characterized in terms of microstructure, using the scanning electron microscopy (HITACHI S2600N electronic microscope).

In all shown images (Figure 7 – Figure 13) it can be seen that the particles from the studied samples do not grow much during the sintering process, their dimensions not exceeding 250 nm.

The samples rich in  $\text{SnO}_2$  (80%) show a reduced ability to sinter, presenting a morphology characteristic for unsintered samples, with noticeable clusters of very fine particles. However,

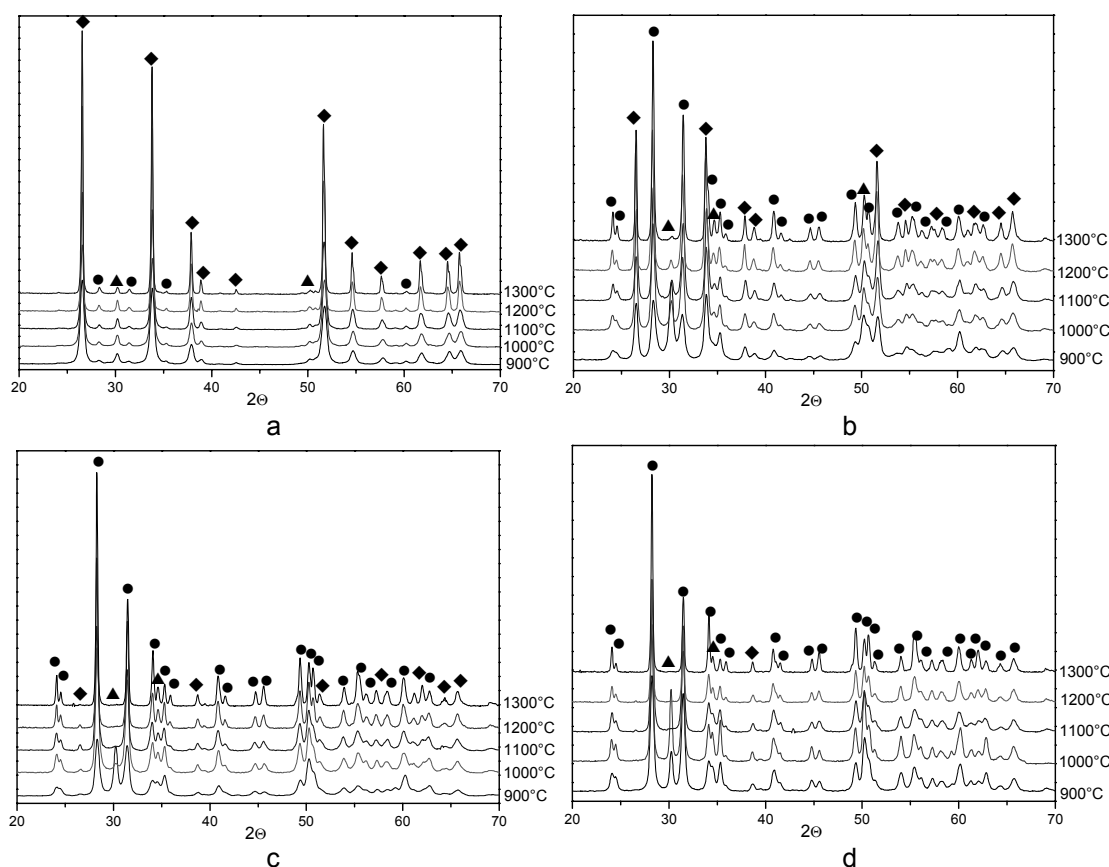


Fig. 6 - X-ray diffraction spectra of the sintered samples/ Spectre de difracție de raze X ale probelor sinterizate la:  
a. Z2S8; b. Z4S6; c. Z6S4; d. Z8S2  
(● -  $\text{ZrO}_2$  tetragonal (ASTM 79-1679); ▲ -  $\text{ZrO}_2$  cubic (ASTM 81-1551); ◆ -  $\text{SnO}_2$  (ASTM 01-0657)).

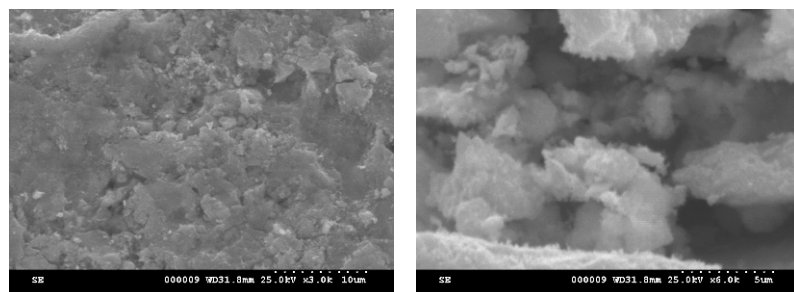


Fig. 7 - SEM images for Z2S8 sample, sinterized at 900°C.  
Imagini MEB pentru proba Z2S8 sinterizată la 900°C.

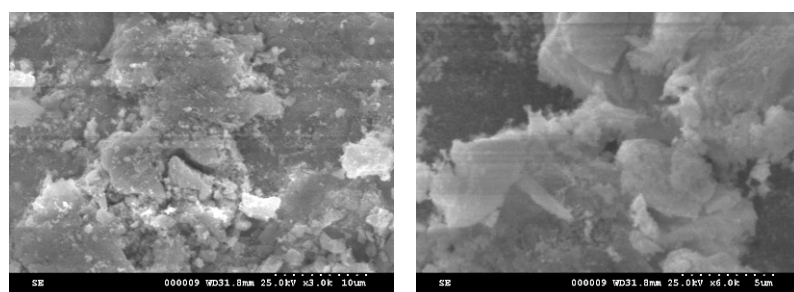


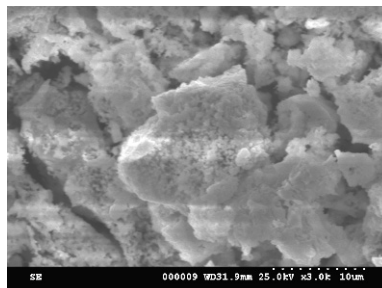
Fig. 8 - SEM images for Z2S8 sample, sinterized at 1100°C.  
Imagini MEB pentru proba Z2S8 sinterizată la 1100°C.

an increase in particle size of ceramic components is remarked with temperature increasing [9].

However, the samples with 80%  $\text{ZrO}_2$  show a higher sintering ability, resembling a consolidated body. At 1300°C, the samples have a completely sintered aspect.

#### 4.3. Ceramic properties

For the samples sintered at temperatures between 900°C and 1300°C, specific ceramic properties were determined - bulk density, relative density,



absorption and open porosity. The results, graphically processed, as shown in the Figure 14.

It can be noticed a difference in behavior for the selected compositions, the samples with a higher amount of  $\text{ZrO}_2$  showing the highest relative densities. As a result of the high degree of sintering, the open porosity of the samples with a greater amount of zirconia shows the smallest values at the highest sintering temperatures.

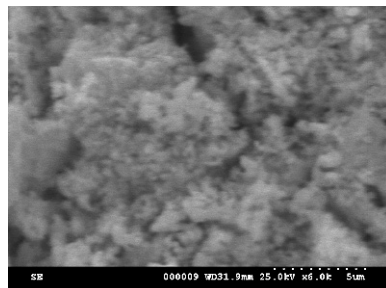


Fig. 9 - SEM images for Z2S8 sample, sinterized at 1300°C.

*Imagini MEB pentru proba Z2S8 sinterizată la 1300°C.*

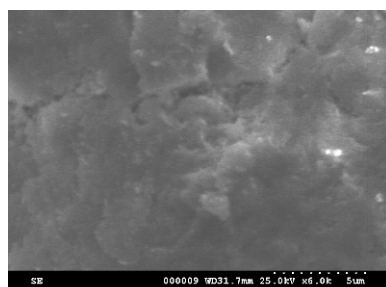


Fig. 10 - SEM images for Z8S2 sample, sinterized at 900°C.

*Imagini MEB pentru proba Z8S2 sinterizată la 900°C.*

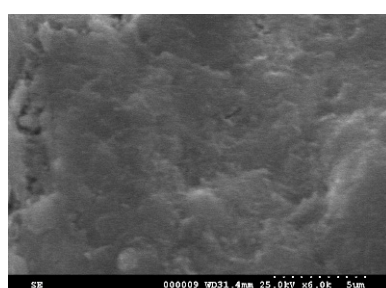
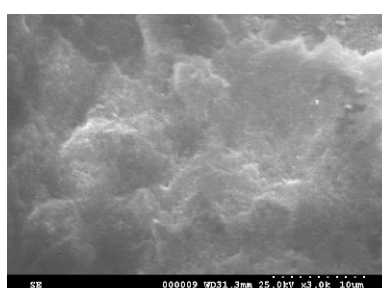


Fig. 11 - SEM images for Z8S2 sample, sinterized at 1100°C.

*Imagini MEB pentru proba Z8S2 sinterizată la 1100°C.*

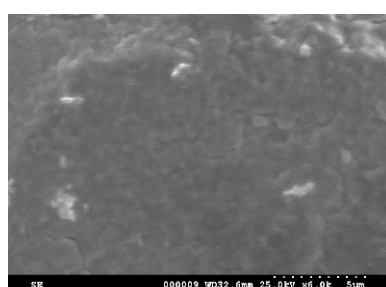
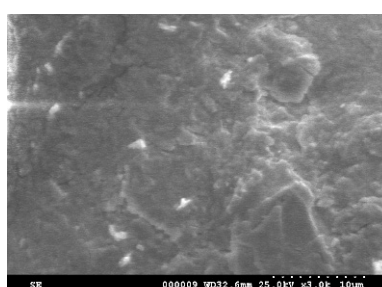


Fig. 12 - SEM images for Z8S2 sample, sinterized at 1300°C.

*Imagini MEB pentru proba Z8S2 sinterizată la 1300°C.*

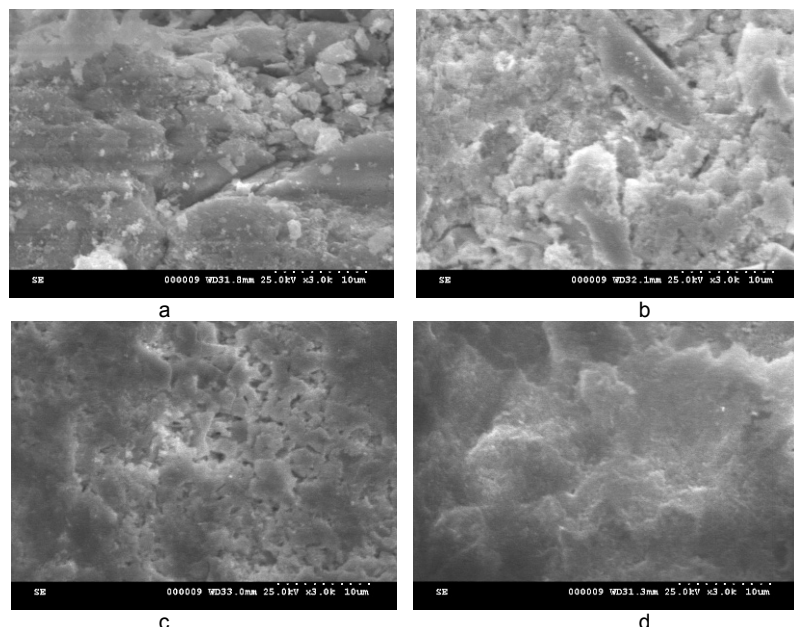


Fig. 13 - SEM images for all four samples, sinterized at 1100°C / Imagini MEB pentru toate patru probele, sinterizate la: a. Z2S8; b. Z4S6; c. Z6S4; d. Z8S2.

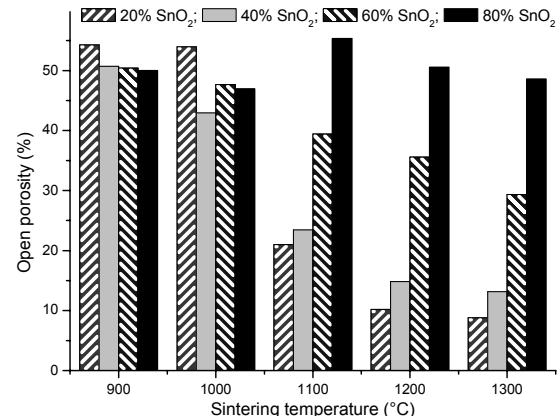
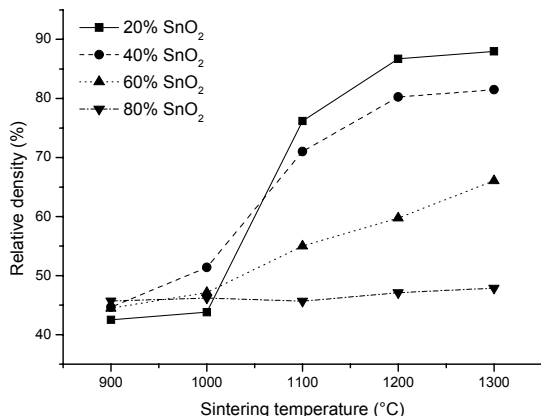


Fig. 14 - Relative density and open porosity as a function of sintering temperature / Densitatea relativă și porozitatea deschisă în funcție de temperatura de sinterizare.

#### 4.4. Sensitivity properties

For all samples sintered from nanometric powders, the electrical resistance was measured in order to determine the sensitivity of the ceramic bodies used as sensors.

Electrical resistances were measured in methane saturated atmosphere and in methanol vapor saturated atmosphere, as well.

Sensitivity was calculated as ratio of the electrical resistance measured in air and the electrical resistance measured in the considered gas [7]. A higher value of this ratio corresponds to a higher efficiency of the sensor.

$$\text{Sensitivity} = \frac{R_{\text{air}}}{R_{\text{gas}}} \quad (1)$$

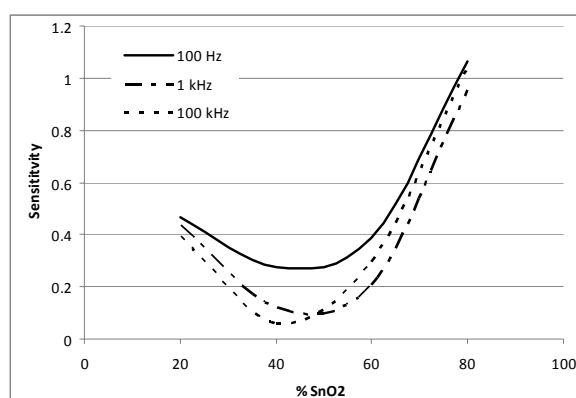
Adsorption of gaseous species on a semiconductor surface produces the appearance of some surface states. Consequently, the electrical properties of these surfaces change due to adsorption and/or chemical reaction [10].

Electrical resistance of samples in analyzed gases was always lower than their electrical resistance measured in air, due to the occurrence of the ionic conduction phenomenon, characteristic both to tin oxide and stabilized zirconium oxide.

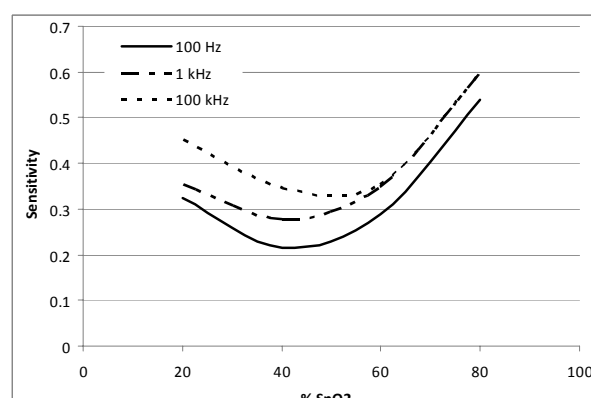
The curves for sensitivity to methane show a better behavior for samples that contain the highest amount of tin, in this case being registered the highest values for sensitivity (Figure 15). It can be stated that the variation of the measurement frequency does not influence the resistance measured which is not following a specific pattern, thus a criterion of influence has not been able to be elaborated

However, it can be noted that for all considered sintering temperatures, there is a composition that shows the lowest sensitivity (with 40%  $\text{SnO}_2$ ).

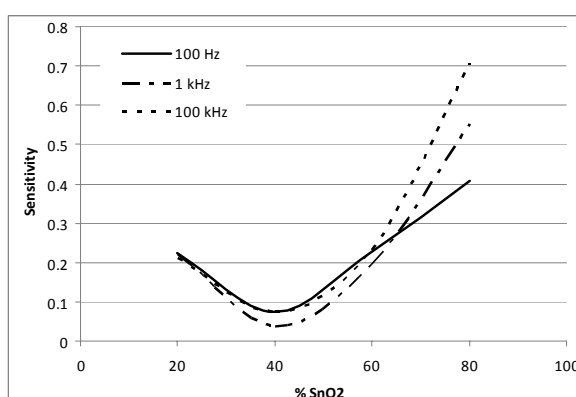
Regarding the sensitivity towards methanol of the obtained ceramic materials, it can be



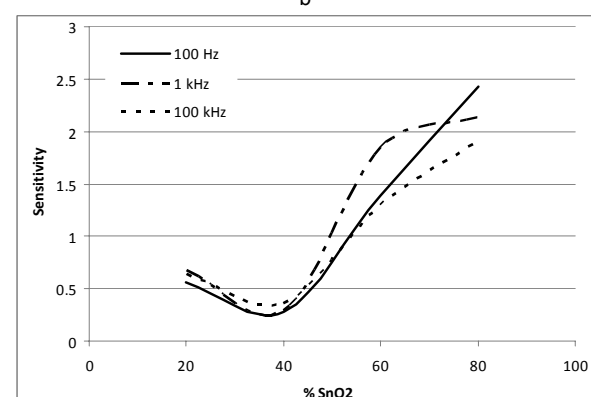
a



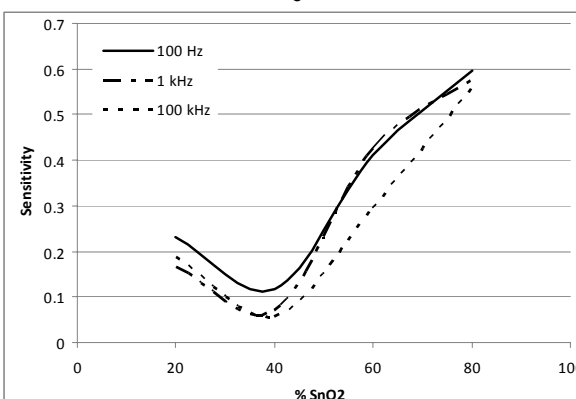
b



c

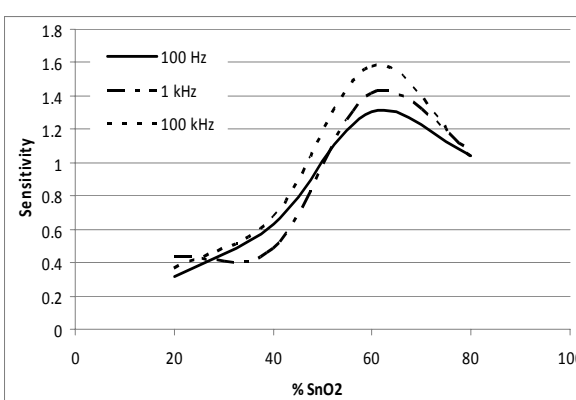


d

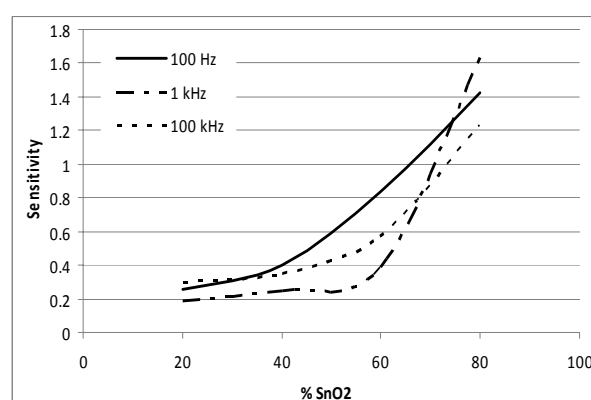


e

Fig. 15 - The sensor sensitivity obtained in methane  
Sensibilitatea senzorului obținută în metan :  
a –  $900^\circ\text{C}$ , b –  $1000^\circ\text{C}$ , c –  $1100^\circ\text{C}$ , d –  $1200^\circ\text{C}$ , e –  $1300^\circ\text{C}$ .



a



b

Fig. 16 continues on next page / continuă pe pagina următoare

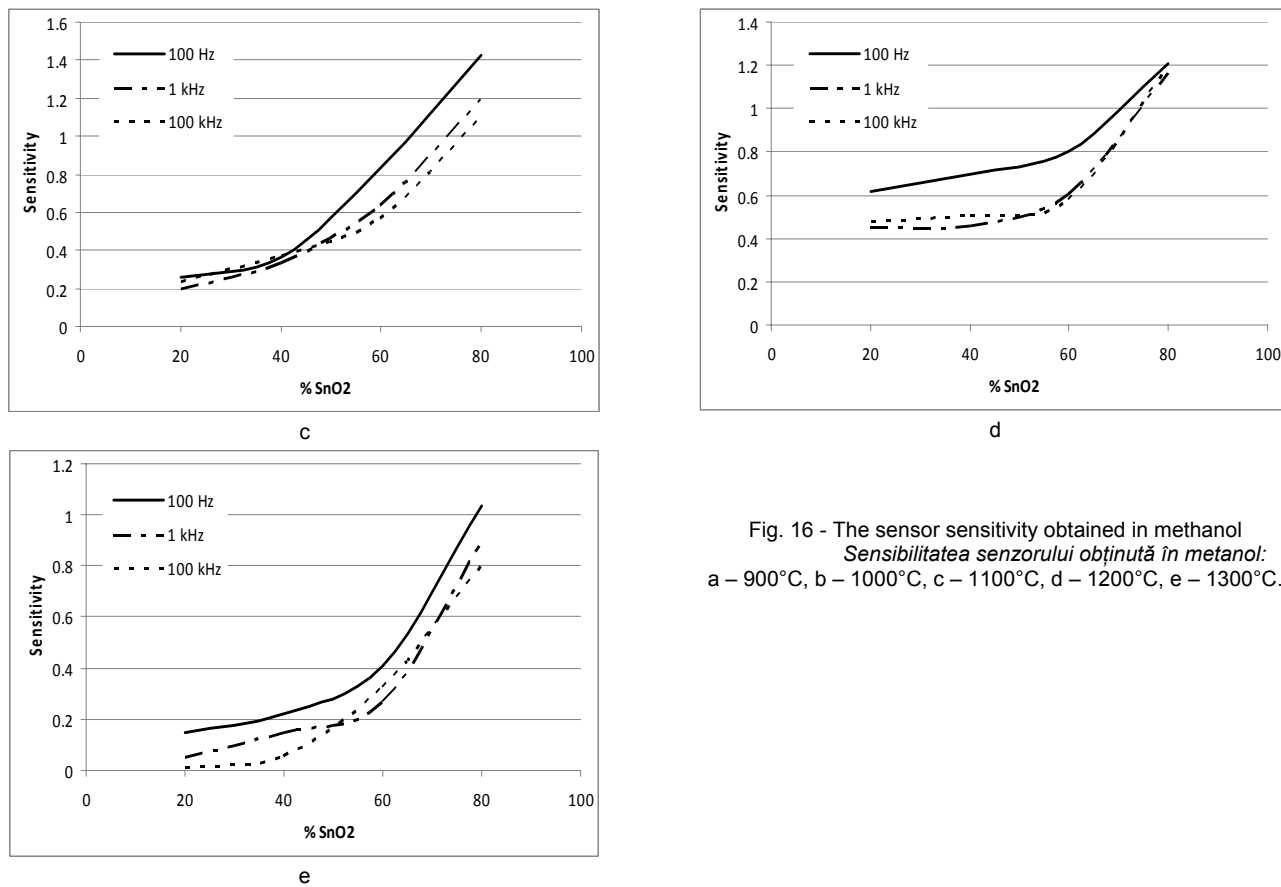


Fig. 16 - The sensor sensitivity obtained in methanol  
Sensibilitatea senzorului obținută în metanol:

a – 900°C, b – 1000°C, c – 1100°C, d – 1200°C, e – 1300°C.

ascertained that they are far more sensitive, reaching higher sensitivity values than the ones normally registered; sensitivity increases with the increase of tin oxide proportion in the analyzed samples (Figure 16).

These generally higher sensitivity values can be justified by the adsorption phenomenon of the alcohol molecules on the ceramics surfaces, this contributing to the increase of overall conductivity and thus to the decrease of electrical resistance.

## 5. Conclusion

The following conclusions can be drawn from this study:

- Through a simple method of precipitation from chlorides, nanometric particles of sizes below 10 nm can be obtained.
- The sensors with a larger amount of tin oxide exhibit a low ability to densify - high values of the open porosity, thus a higher sensitivity.
- The obtained sensors are more sensitive to methanol than to methane, the compositions with a higher amount of tin oxide showing higher sensitivity values to both methanol and methane.

## Acknowledgements

This paper is supported by the Sectorial Operational Programme Human Resources Development, financed from the European Social Fund and by the Romanian Government under the contract number POSDRU/86/1.2/S/58146 (MASTERMAT)

## REFERENCES

1. V. Suciu, M. and V. Suciu, The study of materials, Fair Parteners, Publishing House, Bucharest, 2007.
2. S. Mihaiu, O. Scarlat, S. Zuca, and M. Zaharescu, Advanced SnO<sub>2</sub>-based ceramics: synthesis, structure, properties, Ed. InTech, 2011.
3. M. Batzill, and U. Diebold, The surface and materials science of tin oxide, Progress in Surface Science, 2005, **79**, 47.
4. O. F. Caltun, M. Căldăraru, and C. Munteanu, Magnetostrictive cobalt ferrites, Alexandru Ioan Cuza University Publishing House, Iași, 2008.
5. H.N. Lim, R. Nurzulaikha, I. Harrison, S.S. Lim, W.T. Tan, and M.C. Yeo, Spherical tin oxide, SnO<sub>2</sub> particles fabricated via facile hydrothermal method for detection of Mercury (II) ions, Int. J. Electrochem. Sci., 2011, **6**, 4329.
6. Z. Wang, Z. Li, L. Liu, X. Xu, H. Zhang, W. Wang, W. Zheng, and C. Wang, A novel alcohol detector based on ZrO<sub>2</sub>-doped SnO<sub>2</sub> electrospun nanofibers, J. Am. Ceram. Soc., 2010, **93** (3) 634.
7. G. Fang, Z. Liu, Z. Zghang, and K.-Lunyao, Preparation of ZrO<sub>2</sub>-SnO<sub>2</sub> Thin Films by the Sol-Gel Technique and Their Gas Sensitivity, Physica Status Solidi (A) 1996, **156**, 81.
8. T.A. Miller, S.D. Bakrania, C.Perez, and M.S. Wooldridge, Nanostructured tin dioxide materials for gas sensor applications, Functional Nanomaterials, 2006.
9. S. Mihaiu, O. Scarlat, M. Zaharescu and J. Groza, SnO<sub>2</sub>-based ceramics densified by different sintering methods, Romanian Journal of Materials, 2005, **35** (4), 275.
10. Z. Chen, and C. Lu, Humidity Sensors: A review of materials and mechanism, Sensor Letters 2005, **3**, 274.